JOURNAL OF MATERIALS SCIENCE 29 (1994) 1368–1373

XPS and corrosion studies on zinc phosphate coated 7075-T6 aluminium alloy

W. F. HEUNG, Y. P. YANG, P. C. WONG, K. A. R. MITCHELL
Department of Chemistry, University of British Columbia, 2036 Main Mall, Vancouver, British Columbia, Canada V6T 1Z1

T. FOSTER
Chemistry Group, Defence Research Establishment Pacific, FMO Victoria, British Columbia, Canada V0S 1B0

X-ray photoelectron spectroscopy (XPS), combined with scanning electron microscopy (SEM), weight loss tests and atomic absorption spectroscopy (AAS), has been applied to investigate the corrosion protection properties of zinc phosphate when coated on 7075-T6 aluminium alloy. XPS is consistent with the coating process leading to both physically adsorbed and chemically absorbed zinc. The former is washed away by ultrasonic washing, but the chemically absorbed component, identified as ZnO_x, is incorporated into the aluminium oxide layer. This layer helps suppress the dissolution of aluminium during the corrosion process.

1. Introduction

Aluminium alloys have long been used in the aircraft and automobile industries because of their high strength-to-weight ratio and high durability [1]. The naturally formed oxide film on the aluminium surface provides corrosion resistance, but its thickness may vary due to variations in alloy composition, surface cleanliness and atmospheric exposure; also this film can provide an unreliable base for the application of paints and adhesives. Various methods, including chemical conversion coatings, anodizing and electrolytic and chemical polishing are available to control the thickness of the oxide film, increase the corrosion resistance of the aluminium surface, and improve the adhesion of coatings and adhesives. Zinc chromate has been widely used in chemical conversion coatings as well as a pigment in anti-corrosive primers; in both cases the zinc chromate increases the corrosion resistance of the aluminium surface. However, toxicity studies [2, 3] have indicated that zinc chromate is a carcinogen, and its use in chemical conversion coatings and as a pigment in anti-corrosive primers is consequently being restricted. In turn, replacement pigments and treatment processes are being developed and evaluated.

To aid the search for materials which can act as possible replacement pigments and conversion coatings for zinc chromate, it would be useful to establish the mechanism of interaction of the various pigments with the aluminium surface and the mechanism of corrosion protection. One material under consideration as a replacement for zinc chromate is zinc phosphate ($Zn_3(PO_4)_2$), which has become established in a pretreatment process for steel [4, 5] and has also been applied as a pretreatment for aluminium. Indeed, zinc phosphate, in combination with other pigments, has been used to develop new wash (etch) and marine primers for both aluminium and steel [6].

In this work, X-ray photoelectron spectroscopy (XPS) has been employed to study and characterize the chemical compositions and structures of surface oxide layers on a 7075-T6 aluminium alloy after treatment with zinc phosphate. The effects of exposure to a corrosive environment (3.5% sodium chloride) have also been studied by XPS; additionally the corrosion protection performance of this treatment has been evaluated by making characterizations with scanning electron microscopy (SEM), weight loss measurements and atomic absorption spectroscopy (AAS).

2. Experimental procedure

Studies were done on square test panels of 7075-T6 aluminium alloy ([1] pp.86–7) of side 1 cm and thickness 0.12 cm. The samples used for SEM and XPS analyses were all polished to a mirror-like appearance (0.03 μm finish) to help identify any changes occurring after later treatments. For weight loss measurements, the whole of a test panel (two faces and four edges) was polished to a 220 grit finish. After polishing, all panels were degreased with acetone and methanol. The coating process was done by suspending these test panels in 10% zinc phosphate (ZPO) solution for 1 h at room temperature. After coating, the panels were normally ultrasonically rinsed in distilled water for 1 min, followed by rinsing with absolute ethanol and then air-dried, but XPS analyses were done on panels with and without the ultrasonic rinsing.

0022–2461

Scanning electron micrographs at 4000 magnification were measured in a Hitachi S-2300 model microscope operated at 5 kV. Corrosion rates were determined from weight loss measurements according to the method detailed in ASTM G1-81 [7]. These studies were done on both blank and coated panels when separately immersed in a 3.5% sodium chloride (NaCl) solution for 2 h. AAS was used for detecting the presence of Al^{3+} dissolved in NaCl solutions after the weight-loss test. The absorbance was measured at 309.21 nm wavelength in a Perkin–Elmer 305A spectrometer with the N_2O/acetylene flame in operation. Corrections were made for NaCl interference in the background.

XPS spectra were measured in a Leybold MAX200 spectrometer at an operating pressure of 6×10^{-9} mbar. The unmonochromatized MgK_α radiation source (1253.6 eV) was operated at 15 kV and 20 mA. Survey spectra, for use in qualitative analysis, were obtained with the pass energy of the hemispherical analyser set at 192 eV; higher resolution narrow-scan spectra were measured for the Zn 2p, O 1s, C 1s and Al 2p core levels at a 48 eV pass energy. For the latter, integrated peak areas determined after background subtraction were taken to measure relative elemental amounts after correction with the appropriate sensitivity factors provided by the manufacturer. Core level binding energies were referenced to the gold $4f_{7/2}$ binding energy at 84.0 eV. Narrow scan spectra were also measured for different values of the take-off angle, θ, which is defined as the angle between the plane of the sample surface and the axis of the detector. The latter measurements are helpful to offer surface morphology and indicate composition–depth profiles by non-destructive means [8, 9].

3. Results

3.1 XPS studies

Five differently treated samples (designated A–E) were examined with XPS, and the sample codes are identified in Table I. Briefly, sample A is the blank 7075-T6 aluminium panel, sample B is the same sample after exposure to the corrosive environment, sample C is ZPO-coated aluminium panel after ultrasonic rinsing in water, sample D is the same sample after exposure to the corrosive environment, and sample E is like C except no ultrasonic rinsing is done. Fig. 1 compares survey spectra for samples A and C; the latter shows the presence of zinc in addition to oxygen, carbon and aluminium. Fig. 2 shows the Zn $2p_{3/2}$ peak at high resolution for samples C and E at take-off angles of

TABLE I Identification of samples studied with XPS

Code	Sample identification
A	Polished 7075-T6 aluminium panel
B	Sample A after immersion in 3.5% NaCl solution for 2 h
C	Sample A after treating with 10% ZPO solution for 1 h followed by an ultrasonic rinse in distilled water
D	Sample C after immersion in 3.5% NaCl solution for 2h
E	Sample A after treating with 10% ZPO solution for 1 h (i.e. no ultrasonic rinse in water)

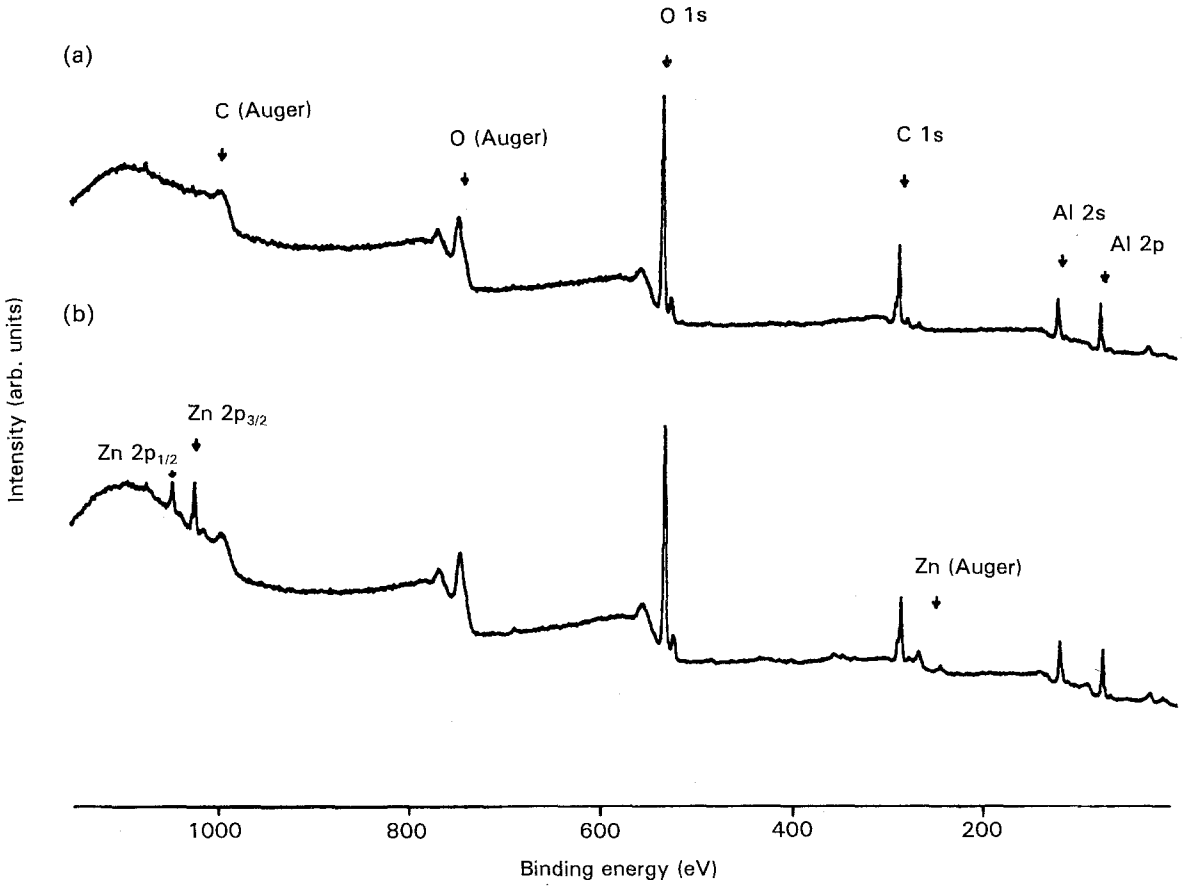

Figure 1 XPS survey scan spectra of the aluminium panel: (a) blank (sample A); (b) ZPO-coated (sample B).

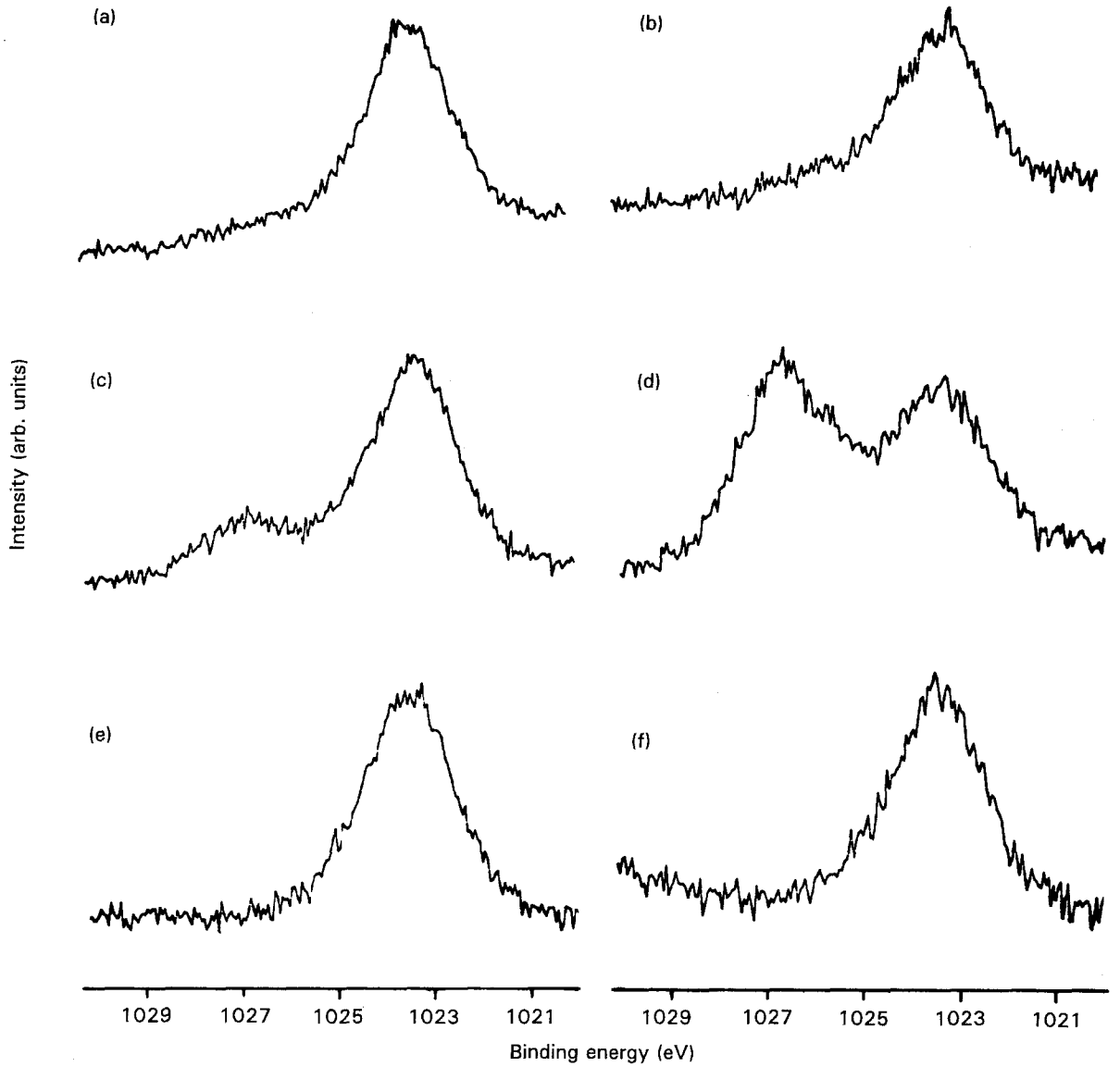

Figure 2 Zn $2p_{2/3}$ spectra for (a) sample C, $\theta = 90°$, (b) sample C, $\theta = 30°$; (c) sample E, $\theta = 90°$; (d) sample E, $\theta = 30°$; (e) sample E, $\theta = 90°$ after bias potential; (f) sample E, $\theta = 30°$ after bias potential.

90° and 30°. It is clear that two forms of zinc are present in sample E, with binding energies of 1026.7 and 1023.3 eV, but only the second is well-established in sample C, which has been ultrasonically washed after the ZPO-treatment. The variations with θ show that the 1026.7 eV peak is in the very topmost region; also even for sample E this peak is effectively removed when the bias potential technique [10] is applied. This involved making measurements with a negative bias potential (− 94.3 eV) applied to the sample, and then shifting the measured spectrum back by 94.3 eV. Nevertheless, the negative bias potential technique has no effect on the lower binding energy component, which still lies at 1023.3 eV after the measured spectrum is shifted back (Fig. 2e–f). For the latter component, the sum of the Auger parameter, α (α = kinetic energy of Zn $L_3M_{45}M_{45}$ Auger electron-kinetic energy of Zn $2p_{3/2}$ electron), and the excitation source energy (1253.6 eV) equals 2010.0 eV, which is consistent with that component arising from an oxide ZnO_x [11].

Survey spectra of samples B and D, after immersing in NaCl solution, show the presence of aluminium, zinc, oxygen and carbon, but interestingly, sodium and chloride are not detected. Both samples A and C show the presence of AlO_x at a binding energy of 74.1 eV and metallic aluminium at 71.5 eV. The composition ratio of the oxide peak to the metallic peak for $\theta = 90°$ is about 15:1, and this ratio increases with decreasing take-off angle; this matches the conventional expectation that the oxide layer is on top of the bulk metal [12]. Also, using the approach of Massies and Contour [13], the thicknesses of the oxide layers are estimated at around 3.6 and 4.6 nm for samples A and C, respectively, using mean free path values estimated from Seah and Dench [14]. For samples B, and D, the Al 2p spectra show only the oxide peak, an observation which is consistent with these samples having a further oxidation of aluminium metal to AlO_x in the salt solution. For sample B, the Zn $2p_{3/2}$ spectrum shows a small peak corresponding to the binding energy of 1023.3 eV. This component is not seen in the corresponding spectrum for sample A, and these two observations suggest that an effect of the immersion in NaCl solution is to expose some oxidized zinc from the bulk alloy (zinc is nominally present at around the 5% level in the 7075-T6 sample

TABLE II Zn/AlO_x composition ratios from samples A–D estimated at different take-off angles, θ

θ (deg)	Zn/AlO_x composition ratio			
	A	B	C	D
30	0.000	0.008	0.050	0.092
45	0.000	0.016	0.065	0.067
60	0.000	0.015	0.073	0.063
90	0.000	0.017	0.076	0.064

([1] pp. 86–7). Table II summarizes the zinc to AlO_x composition ratio estimated for different take-off angles for samples A to D.

3.2. Corrosion studies

Fig. 3a–d show scanning electron micrographs for samples A–D, respectively. Prior to the immersion in the NaCl solution, both sample A (the blank) and sample C (the ZPO-treated surface) had a similar flat appearance under the SEM (Fig. 3a and c, respectively). After exposure to the salt solution, the untreated aluminium sample (B) showed a large corroded area (Fig. 3b), but the corroded areas on the ZPO-treated sample D were much less (Fig. 3d). Corrosion rates for samples A and C were estimated by weight-loss measurements. After the 2 h immersion in the salt solution, the corrosion rate for the untreated sample was found to be 118 $\mu g\,m^{-2}\,s^{-1}$, although no weight loss was detected for sample C. Correspondingly, AAS measurements, to detect the presence of aluminium ions in the solution after the weight-loss measurements, showed about 0.2 p.p.m. in solution from the blank sample A, but from the ZPO-treated sample C, the aluminium content in solution was below the detection limit of 0.01 p.p.m.

4. Discussion

The XPS observations for samples C–E make it clear that zinc adsorbs on the 7075-T6 aluminium alloy surface during the ZPO-coating process, although no phosphorous is detected by this technique for the sample treatments used. The contrast between Zn $2p_{3/2}$ spectra of samples C and E emphasizes the two distinct forms of zinc bonding. The effect of the bias potential applied to sample E suggests that the component associated with the 1026.7 eV binding energy is not in electrical contact with the metal [10], although this conclusion contrasts with the situation for the zinc associated with the 1023.3 eV binding energy. It is concluded that the 1026.7 eV component corresponds to zinc that is weakly bonded (physically trapped) at the surface (hence it can be lost by ultrasonic washing), whereas the ZnO_x component at 1023.3 eV binds strongly at the surface.

No zinc was detected initially by XPS on the blank aluminium alloy surface (sample A), although after

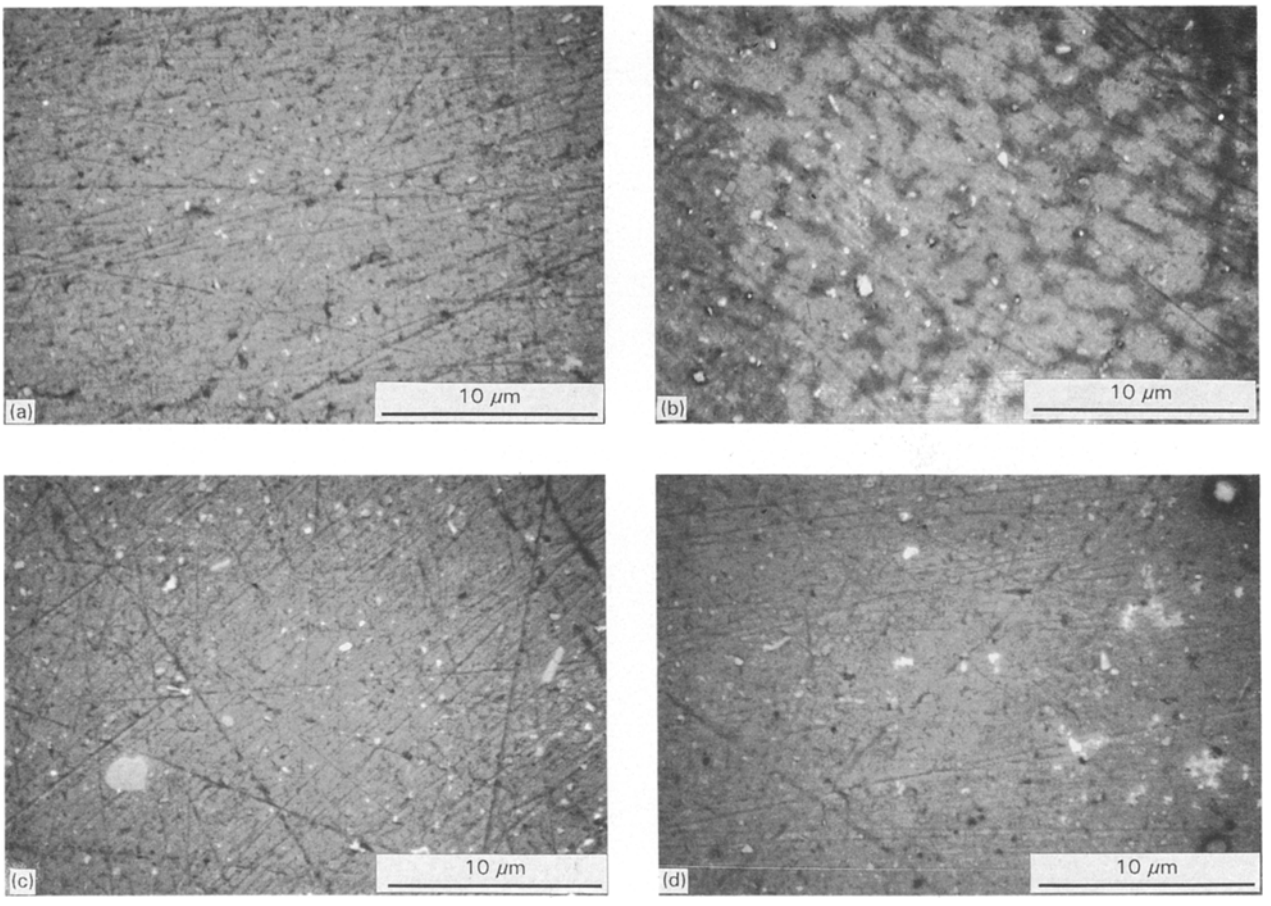

Figure 3 Scanning electron micrographs of (a) sample A, (b) sample B, (c) sample C, (d) sample D.

exposure to the NaCl solution, a compound interpreted as ZnO_x was found; this appears to originate from the zinc in the alloy. On this interpretation there has clearly been some AlO_x dissolution, which is consistent with the results obtained from weight loss and AAS measurements. The Zn/AlO_x ratio for sample B (Table II, column 2) shows an essentially angle-independent behaviour for θ in the range 45°–90°, and this suggests that the ZnO_x is distributed reasonably homogeneously with the AlO_x [9]. The slightly lower value for $\theta = 30°$ (but the difference is barely significant) may suggest that relatively there is slightly less zinc in the very topmost region. There is a significant increase in the Zn/AlO_x ratio from sample A to sample C, and this confirms the absorption of zinc from the coating process. Again, from the ratio for $\theta = 30°$, there appears to be slightly less zinc at the topmost surface compared with the region just below. Also, the ZnO_x still appears to be distributed reasonably homogeneously within the AlO_x [9], and Fig. 4 schematically indicates the morphology suggested for the ZPO-treated alloy surface. The Zn/AlO_x ratios are similar for samples C and D over the range of θ from 45°–90°, but for $\theta = 30°$ relatively more zinc is seen in sample D. This suggests that the effect of the NaCl solution treatment is to effectively build up ZnO_x on the surface by the preferential removal of AlO_x. However, overall, the ZPO coating process acts to reduce the alloy corrosion rate.

The common point observed in previous studies of chloride attack on naturally formed and anodized aluminium oxide-covered aluminium is the dissolution of the metal [15–18], which is also observed in the present research. Nguyen and Foley [15, 17,18] proposed the following mechanism:

Step 1 Adsorption on the oxide film

$$Cl^-(\text{in bulk solution}) \rightarrow Cl^- (\text{adsorbed on } Al_2O_3 \cdot H_2O \text{ sites}) \quad (1)$$

Step 2 Chemical reaction

$$Al^{3+} (\text{in } Al_2O_3 \cdot H_2O \text{ lattice}) + 2Cl^- + 2OH^- \rightarrow Al(OH)_2Cl_2^- \quad (2)$$

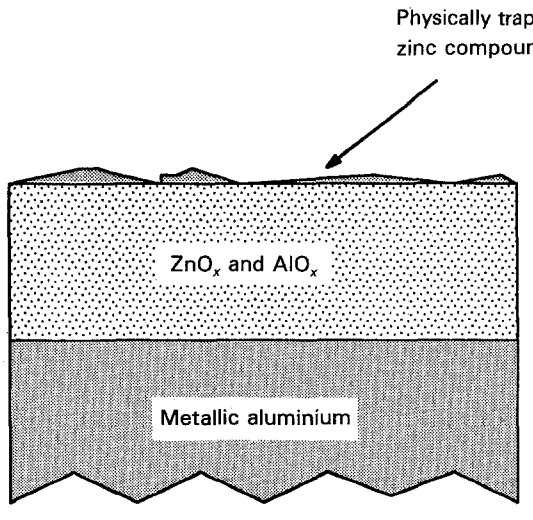

Figure 4 A schematic indication in cross-section for the ZPO-treated aluminium panel surface region.

The product $Al(OH)_2Cl_2^-$ is a soluble complex which is proposed to diffuse from reaction sites into solution. In the meantime, oxidation of the metallic aluminium occurs [17, 18]

$$Al + 3H_2O \rightarrow Al(OH)_3 + 3H^+ + 3e \quad (3)$$

The results in the present work are consistent with this mechanism. Breakdown of the oxide film by Cl^- causes a rough and corroded surface appearance according to SEM investigation. The aluminium complex dissolving from the solid (Reaction 2) contributes to the aluminium detected by AAS. Reaction 2 is also consistent with the XPS observation that no Cl^- is detected on the 7075-T6 aluminium alloy surface after the corrosion test, which was first reported by Arnott *et al.* [19]. Consistently with our observations, these authors also failed to detect zinc on the blank surface, but confirmed its presence after the corrosion test. The dissolution of aluminium from the ZPO-treated surface is greatly suppressed. Possibly the zinc strengthens the surface lattice structure and thereby slows down the aluminium dissolution.

5. Conclusions

1. XPS indicates that treatment of 7075-T6 aluminium alloy by zinc phosphate (ZPO) solution results in the first instance in two forms of zinc bonded to the surface. One is weakly bound, and can be removed by ultrasonic washing, but the other is strongly bound and is interpreted to correspond to an oxide ZnO_x.

2. The ZnO_x formed by the ZPO treatment is distributed reasonably homogeneously within the aluminium oxide film above the metal.

3. The ZPO treatment increases alloy stability in a corrosive Cl^- solution environment as shown by SEM, weight loss and AAS measurements, as well as XPS.

4. XPS observations of corroded samples are consistent with Cl^- attack according to the mechanism proposed by Nguyen and Foley.

Acknowledgements

We acknowledge support for this research by the Defence Research Establishment Pacific and by the Natural Sciences and Engineering Research Council of Canada.

References

1. F. KING, "Aluminium and its Alloys" (Ellis Horwood, Chichester, 1987) Ch. 9.
2. F. de L. FRAGATA and J. E. DOPICO, *Surf. Coat. Int.* **74** (1991) 92.
3. P. A. SCHWEITZER, "Corrosion and Corrosion Protection Handbook" (Marcel Dekker, New York, 1988) Ch. 4.
4. T. FOSTER, G. N. BLENKINSOP, P. BLATTLER and M. SZANDOROWSKI, *J. Coat. Technol.* **63** (1991) 91.
5. A. TURUNO, K. TOYOSE and H. FUJIMOTO, *Kobelco Tech. Rev.* **11** (1991) 14.
6. T. FOSTER, G. N. BLENKINSOP, P. BLATTLER and M. SZANDOROWSKI, *J. Coat. Technol.* **63** (1991) 101.
7. 1985 Annual Book of ASTM Standards, Section 3, "Metals Test Methods and Analytical Procedures", (American Society

for Testing and Materials, Philadelphia, PA; 1985) pp 88–93, 176–85.
8. C. S. FADLEY, *Prog. Surf. Sci.* **16** (1984) 275.
9. B. D. RATNER, T. A. HORBETT, D. SHUTTLEWORTH and H. R. THOMAS, *J. Colloid Interface Sci.* **83** (1981) 630.
10. Y. L. LEUNG, M. Y. ZHOU, P. C. WONG, K. A. R. MITCHELL and T. FOSTER, *Appl. Surf. Sci.* **59** (1992) 23.
11. C. D. WAGNER, in "Handbook of X-ray and Ultraviolet Photoelectron Spectroscopy", edited by D. Briggs (Heyden, London, 1977) Ch. 7.
12. C. S. FADLEY, R. J. BAIRD, W. SIEKHAUS, T. NOVAKOV and S. Å. L. BERGSTRÖM, *J. Electron. Spect.* **4** (1974) 93.
13. J. MASSIES and J. P. CONTOUR, *J. Appl. Phys.* **58** (1985) 806.
14. M. P. SEAH and W. A. DENCH, *Surf Interface Anal.* **1** (1979) 2.
15. T. H. NGUYEN and R. T. FOLEY, *J. Electrochem. Soc.* **127** (1980) 2563.
16. Z. A. FOROULIS and M. J. THUBRIKAR, *ibid.* **122** (1975) 1296.
17. T. H. NGUYEN and R. T. FOLEY, *ibid.* **126** (1979) 1855.
18. R. T. FOLEY and T. H. NGUYEN, *ibid.* **129** (1982) 464.
19. D. R. ARNOTT, N. E. RYAN, B. R. W. HINTON, B. A. SEXTON and A. E. HUGHES, *Appl. Surf. Sci.* **22/23** (1985) 236.

Received 19 April
and accepted 26 August 1993